

Subplementary Material

Spectroscopy and photoisomerization of protonated Schiff-base retinal derivatives in vacuo

Anne P. Rasmussen, Elisabeth Gruber, Ricky Teiwes, Mordechai Sheves, and Lars H. Andersen

1 Laser-Power Dependency

Measurements of the fragmentation signal as a function of laser-pulse energy are used to determine the number of photons which are absorbed to induce fragmentation. Figure 1 shows the fragmentation signal as a function of laser-pulse energy. It is found that absorption of a single photon is enough to cause fragmentation of the native PSBR along with the $C_9=C_{10}$ *trans*-locked, and the derivative without the β ionone ring. The $C_{13}=C_{14}$ *trans*-locked is found to dissociate as a result of a mixture of one- and two-photon absorption.

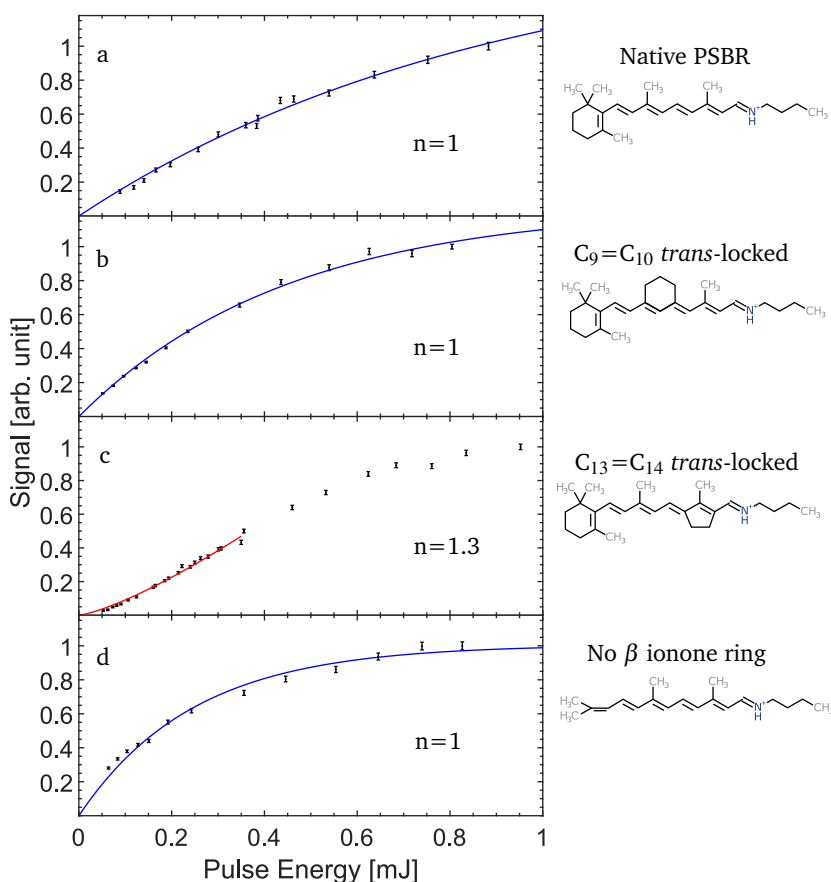


Figure 1 Laser pulse energy dependence measurements of PSBR and the retinal derivatives. **a)** Native all-*trans* protonated Schiff-base retinal, **b)** All-*trans* PSBR locked at $C_9=C_{10}$, **c)** All-*trans* PSBR locked at $C_{13}=C_{14}$, **d)** All-*trans* PSBR without the β ionone ring.

2 Absorption Spectra Measured in Solution

As reference, the solution absorption spectra are measured with an Ocean Optics Flame Spectrometer system. Absorption spectra of the PSBR and the derivatives dissolved in ethanol are presented in figure 2. The absorption of PSBR is blue-shifted in solution-phase compared to gas-phase with a maximum at around 450nm, which has been observed previously.^{1,2} The absorption maximum is unshifted for the C₉=C₁₀ *trans*-locked derivative, while the maximum is slightly red-shifted for the C₁₃=C₁₄ *trans*-locked and derivative without the β ionone ring.

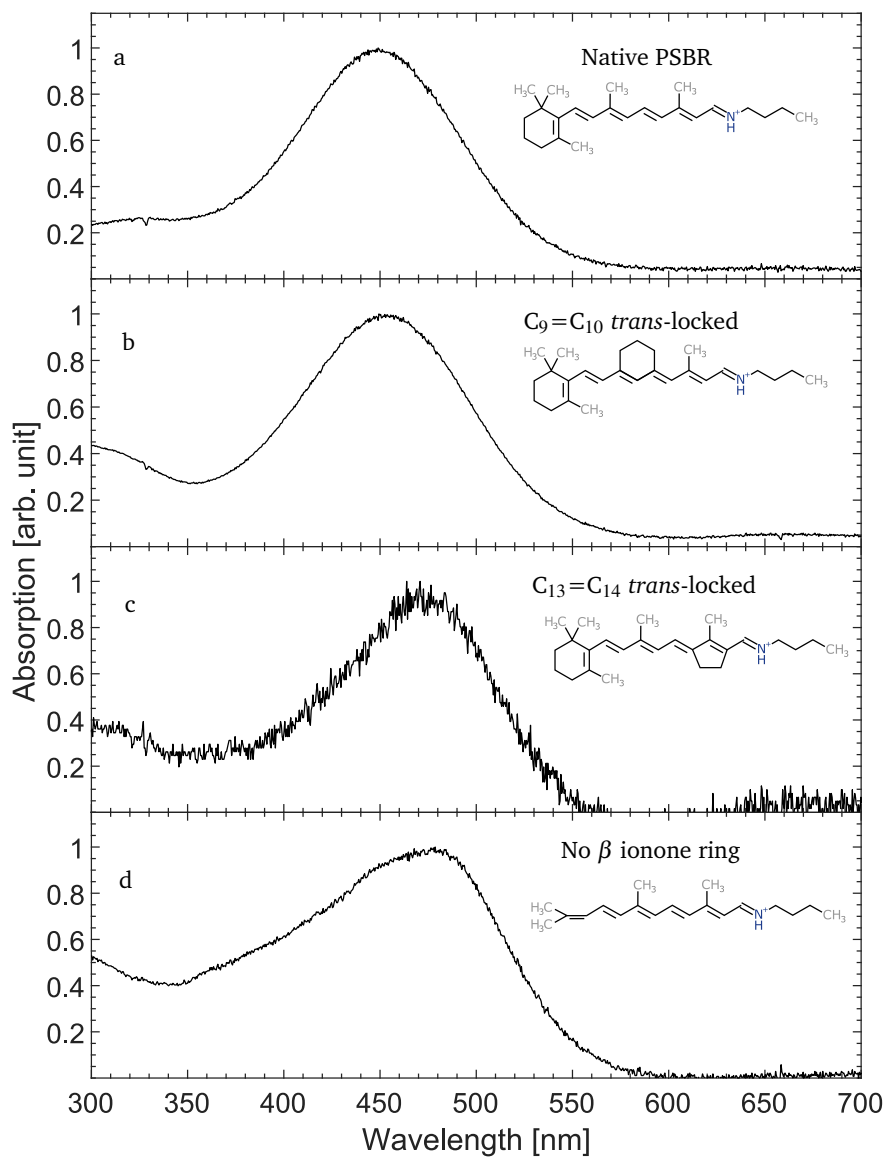


Figure 2 Absorption spectra in solution. The spectra are measured with a Ocean Optics Flame Spectrometer system. **a)** Native all-*trans* protonated Schiff-base retinal, **b)** All-*trans* PSBR locked at C₉=C₁₀, **c)** All-*trans* PSBR locked at C₁₃=C₁₄, **d)** All-*trans* PSBR without the β ionone ring. All samples are dissolved in ethanol and protonated with acetic acid.

3 Evidence for a trapped state in the $C_{13}=C_{14}$ *trans*-locked RPSB derivative

Figure 3 shows the neutral fragment counts for the $C_{13}=C_{14}$ *trans*-locked retinal after laser irradiation at five different wavelengths. The decay becomes faster for lower wavelengths (higher energy) as expected, until around 250nm. Figure 4 shows the total counts per revolution as a function of time after laser irradiation by a 250nm laser pulse. It is clear that the number of fragments initially increase before decreasing. This indicates that the excited ions enter a trapped state from where decay to the ground state is slow. A schematic of the process is shown in figure 5. The excited ions have two competing relaxation branches, both leading into the hot ground state, S_0^* . In one branch, the excited ions undergo internal conversion into the hot ground state. This is a fast process which usually occurs on a fs to ps timescale, which is too fast to be detected at ELISA. In the other branch, the ions enter a trapped state before returning to the ground state. Decay out of the trapped state is for the $C_{13}=C_{14}$ *trans*-locked retinal sufficiently slow that it may be detected at ELISA. The total decay can be describe by

$$\frac{d\vec{N}}{dt} = \begin{bmatrix} -k_{TS} & 0 & 0 \\ k_{TS} & -k_D & 0 \\ 0 & k_D & 0 \end{bmatrix} \cdot \vec{N}, \quad (1)$$

where \vec{N} is an array of the number of ions in the trapped state, the hot ground state, and fragments $\vec{N} = (N_{TS}, N_{S_0^*}, N_F)$. The rate of internal conversion is too fast to be resolved at the ELISA ion-storage ring and is therefore assumed instantaneous in this model. The initial conditions are then $[N_{TS}, N_{S_0^*}, N_F](t=0) = (C_1, C_2, 0)$, where C_1 and C_2 are the initial number of ions in the TS and S_0^* state respectively. The solutions are,

$$N_{T_n} = C_1 \cdot e^{-k_{TS}t} \quad (2)$$

$$N_{S_0^*} = C_2 \cdot e^{-k_D t} - C_1 \cdot \frac{k_{TS}}{k_{TS} - k_D} \left[e^{-k_{TS}t} - e^{-k_D t} \right] \quad (3)$$

$$N_F = C_2 \left[1 - e^{-k_D t} \right] + C_1 \left[1 + \frac{k_D}{k_{TS} - k_D} e^{-k_{TS}t} - \frac{k_{TS}}{k_{TS} - k_D} e^{-k_D t} \right]. \quad (4)$$

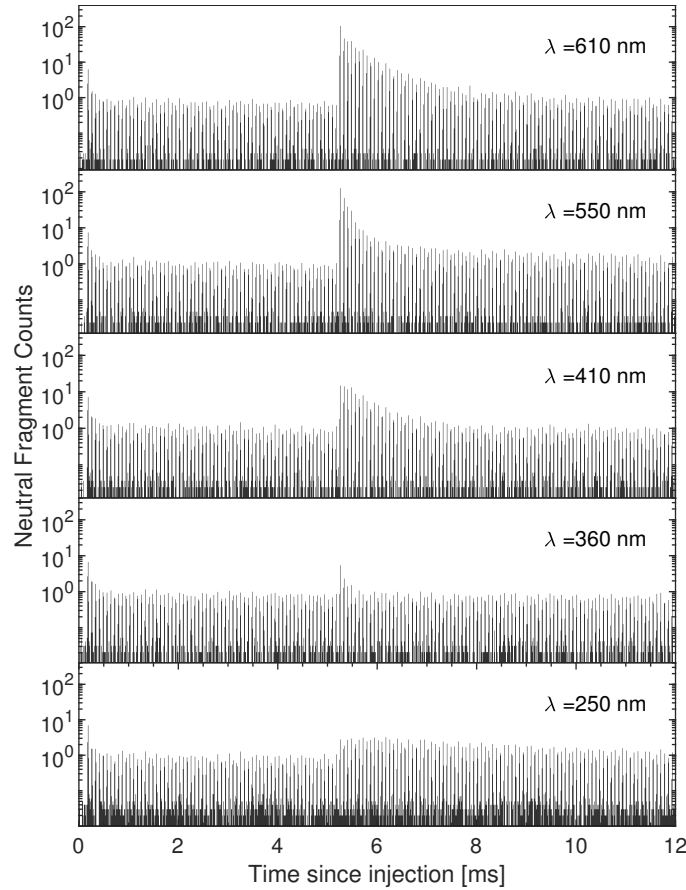


Figure 3 Number of neutral fragments as a function of time after injection measured at different wavelengths for the $C_{13}=C_{14}$ *trans*-locked retinal. Data are obtained in ELISA with ns-laser pulses.

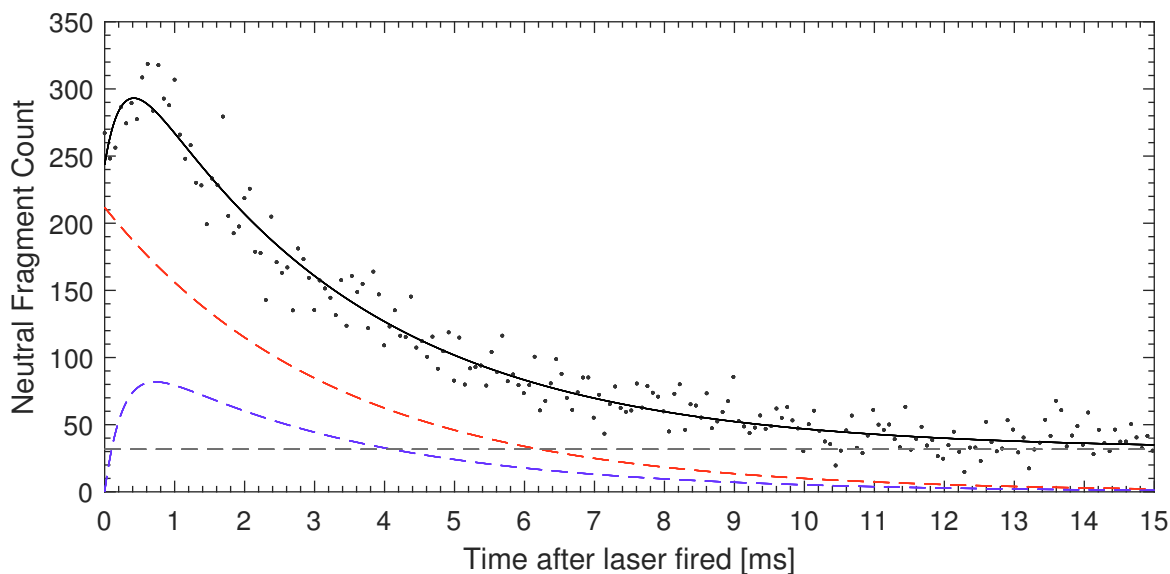


Figure 4 Total number of neutral fragments for each revolution of the ion bunch in the ring as a function of time after laser irradiation by a 250nm laser pulse. The background fragments created by collisions with rest-gas have been subtracted. The black solid line is a fit to the data. The red dashed line represents the fragments formed from ions which directly underwent internal conversion into the hot ground state, while the blue dashed line represents the fragments formed by the ions which entered the trapped state. The revolution time of the $C_{13}=C_{14}$ *trans*-locked retinal in the ELISA storage ring is $77 \mu\text{s}$, which is the spacing between the discrete points.

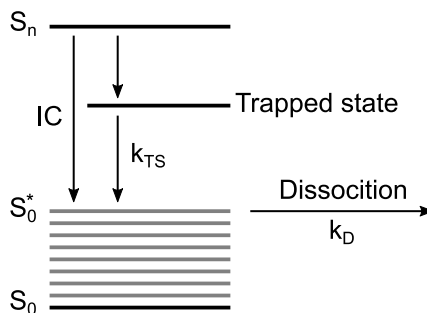


Figure 5 Decay schematic of the $C_{13}=C_{14}$ *trans*-locked retinal. The ions can leave the excited state through internal conversion into a hot ground state or they can enter a trapped state. Exiting the trapped state is slow with a rate k_{TS} . Dissociation occurs from the hot ground state with the rate k_D .

At ELISA we measure the number of fragments as a function of time, $\frac{dN_F}{dt}$:

$$\frac{dN_F}{dt} = k_D \cdot N_{S_0^*}. \quad (5)$$

This function, with an added offset, has been fitted to the decay shown in figure 4. k_D was found to be 0.31 ms^{-1} so the dissociation lifetime is 3.3ms, while k_{TS} was found to be 3.8 ms^{-1} , making the trapped-state lifetime 0.26ms. The trapped state could be a triplet state, accessed through intersystem crossing. Such a decay have previously been documented for chlorophyll.³ Trapping might also occur in the singlet state, which have previously been found in the GFP chromophore.⁴

References

- [1] G. Zgrablić, K. Voitchovsky, M. Kindermann, S. Haacke and M. Chergui, *Biophysical Journal*, 2005, **88**, 2779 – 2788.
- [2] L. H. Andersen, I. B. Nielsen, M. B. Kristensen, M. O. A. El Ghazaly, S. Haacke, M. B. Nielsen and M. Å. Petersen, *Journal of the American Chemical Society*, 2005, **127**, 12347–12350.
- [3] E. Gruber, C. Kjær, S. B. Nielsen and L. H. Andersen, *Chemistry – A European Journal*, 2019, **25**, 9153–9158.
- [4] A. Svendsen, H. V. Kiefer, H. B. Pedersen, A. V. Bochenkova and L. H. Andersen, *Journal of the American Chemical Society*, 2017, **139**, 8766–8771.